Slowly rotating general relativistic superfluid neutron stars with relativistic entrainment

G. L. Comer*
Department of Physics, Saint Louis University, St. Louis, Missouri 63156-0907, USA
(Received 2 February 2004; published 29 June 2004)

Neutron stars that are cold enough should have two or more superfluids or superconductors in their inner crusts and cores. The implication of superfluidity or superconductivity for equilibrium and dynamical neutron star states is that each individual particle species that forms a condensate must have its own, independent number density current and equation of motion that determines that current. An important consequence of the quasiparticle nature of each condensate is the so-called entrainment effect; i.e., the momentum of a condensate is a linear combination of its own current and those of the other condensates. We present here the first fully relativistic modeling of slowly rotating superfluid neutron stars with entrainment that is accurate to the second-order in the rotation rates. The stars consist of superfluid neutrons, superconducting protons, and a highly degenerate, relativistic gas of electrons. We use a relativistic σ-ω mean field model for the equation of state of the matter and the entrainment. We determine the effect of a relative rotation between the neutrons and protons on a star's total mass, shape, and Kepler, mass-shedding limit.

DOI: 10.1103/PhysRevD.69.123009 PACS number(s): 97.60.Jd, 47.75.+f, 95.30.Sf

I. INTRODUCTION

There is now an extended body of evidence in support of superfluidity in dense, nucleonic matter, such as that which is believed to exist in neutron stars. Using conservative estimates one can argue for a Fermi temperature on the order of 10^{12} K for neutrons in media with supranuclear densities, and that the transition temperature to a superfluid state is about 10^9 K. This is a significant fact since it is generally accepted that nascent neutron stars formed from supernovae should cool fairly quickly, and consequently their internal temperatures should pass quickly through the transition value. Observational support for such transitions is supplied by the well established glitch phenomenon in pulsars [1,2]. These are rapid decreases in the rotational periods followed by a slow recovery [3], much too slow to be explained by ordinary fluid viscosity [4]. The best description is based on superfluid quantized vortices, and how they pin, unpin and then repin as the pulsar's rotation rate evolves [5–7]. We present here a fully relativistic formalism to model the rotational properties of superfluid neutron stars within a slow rotation approximation, which is an extension to second order in the rotation rates the previous work of Comer and Joynt [8].

The bulk of the studies of neutron star superfluidity have been in the Newtonian regime, where the intent is not to be quantitatively descriptive but rather to gain qualitative understandings. However, it is becoming increasingly apparent that general relativity is required to obtain even qualitative understandings. And even if the qualitative does not vary between the two regimes, the number of examples is growing where general relativity can yield factors of two difference from Newtonian calculations (as opposed to ''merely'' 20% to 30% corrections). For example, recent modeling of supernovae has revealed that when general relativity is included the range of model parameters that exhibit multiple bounces is significantly smaller than the range found for the Newtonian case [9]. The use of general relativistic hydrodynamics has also led to predictions of the shock radius (during the shock reheating phase) being reduced by a factor of two and a corresponding increase by a factor of two for the inflow speed of the material behind the shock [10]. Certainly the need to use general relativity must only be enhanced as supernova remnants become more compact.

Weber [11] provides an excellent overview of the many suggestions for the matter content of these remnants, the neutron stars. They range from the traditional neutron, proton, and electron models to more exotic configurations with kaon or muon condensates in the core, or hyperons, or even strange stars with absolutely stable *u*, *d*, *s* quark matter. In our study we will be somewhat conservative by considering typical traditional neutron star models, composed of superfluid neutrons, superconducting protons (with proton fractions on the order of 10%), and a highly degenerate relativistic gas of electrons. Each species extends from the center of the star all the way to the surface, although in principle one could consider a more realistic scenario wherein the protons and electrons extend out further than the neutrons [12–14] and in that way mimic features of a crust. This same technique could be applied in neutron star cores, allowing for the possibility of alternating regions of ordinary fluid and superfluid.

The local thermodynamic equilibrium of the matter will be modelled using a relativistic σ-ω mean field approach of the type that is attributed to Walecka [15] and discussed in detail for neutron stars by Glendenning [16]. We consider a relativistic approach to be important on two different levels. On the macroscopic level there is the need for general relativity that was discussed above. But on a microscopic level, recall that any fluid approximation for matter has built into it the notion of local, fluid elements. They are small enough that they can be considered to be points with respect to the rest of the star, and yet large enough to contain, say, an Avogadro's number of particles. At the densities expected for neutron stars, the local, Fermi levels for the nucleons can

*Electronic address: comergl@slu.edu

 ©2004 The American Physical Society

become high enough that the effective velocities of the nucleons with respect to their fluid elements are relativistic. As for the fluid elements themselves, they can also, in principle, approach speeds near that of light, although in practice (e.g. for quasinormal mode [13,17] or slow rotation calculations [8,18]) they will typically have speeds a few percent of that of light.

Because of the superfluidity of the neutrons, and superconductivity of the protons, the fluid formalism to be used differs fundamentally from the standard perfect fluid approach in that the neutrons can flow independently of the protons and electrons. There are thus two fluid degrees of freedom in the system, requiring two sets of fluid elements, one set for the neutrons and another for the charged constituents since the electromagnetic interaction very effectively ''ties'' the electrons to the protons. The matter description, therefore, must take into account two Fermi levels for the nucleons, and a displacement in momentum space between their respective Fermi spheres that will result when one fluid flows with respect to the other. The specification of a local thermodynamic equilibrium for the two fluids requires that the local neutron and ''proton'' (i.e., a conglomeration of the protons and electrons) number densities be known as well as the local, relative velocity of the proton fluid elements, say, with respect to those of the neutrons.

When the Fermi spheres for the nucleons are displaced with respect to each other there results an important effect for neutron star dynamics known as entrainment [19]. Sauls [20] describes the entrainment effect using quasiparticle language, i.e. just because the neutrons are superfluid and protons superconducting does not mean they no longer feel the strong force. On the contrary, an individual neutron should be understood as being surrounded by a polarization cloud of other neutrons and protons. When this neutron moves, it will be accompanied by this cloud of nucleons. The net effect at the level of the fluid elements is that the momentum of a neutron fluid element is a linear combination of the neutron *and* proton number density currents. Parameters that are important for entrainment in neutron stars have been calculated in the Newtonian regime using a Fermi-liquid approach [21] and in the relativistic regime via a σ-ω mean field model [8]. Comer and Joynt [8] find that one of the key parameters that has been much used in superfluid neutron star modeling extends over a much larger range of values than what the Newtonian analysis of Borumand *et al.* would imply [21].

Comer and Joynt also used their formalism to obtain first order rotational corrections to a superfluid neutron star's equilibrium state, which for general relativity means determining the frame-dragging, and the angular momentum. We will extend those calculations to the second order in the rotation rates, and thereby determine rotational corrections to the metric, distribution of particles, the total mass, shape, and the Kepler, mass-shedding limit. We construct sequences of equilibrium configurations where members of the sequence have the same relative rotation between the neutrons and protons but are distinguished by their central neutron number densities. We also construct sequences where the central neutron number density is fixed and the relative rotation is allowed to vary (cf. [12,18] for discussions on when to expect a relative rotation). One other straightforward, but important, extension here of the work of Comer and Joynt is a proof that the matter coefficients obtained by them are sufficient for our second order calculations.

In order to have a reasonably self-contained document, and to define all the variables, we review in Sec. II the general relativistic superfluid formalism and its application to slowly rotating neutron stars. It is in this section that we prove the matter coefficients obtained by Comer and Joynt are all that is needed for the extension to second order. In Sec. III we discuss the highlights of the relativistic σ-ω model and its mean field limit. We also determine the model's slow rotation limit. In Sec. IV we join the slow rotation formalism with the mean field model and produce numerical solutions. After reviewing the main results, the final, concluding section discusses applications beyond those considered here and points out where the formalism should be improved. For convenience we have restated in the appendix results of Comer and Joynt for the various matter coefficients that are required input for the field equations. We use ''MTW'' [22] conventions throughout and geometrical units.

II. GENERAL RELATIVISTIC SUPERFLUID FORMALISM AND SLOW ROTATION

A. The full formalism

We will use the formalism developed by Carter, Langlois, and their various collaborators [17,18,23–30]. The fundamental fluid variables consist of the conserved neutron n^μ and proton p^μ number density currents, from which are formed the three scalars $n^2=-n_\mu n^\mu$, $p^2=-p_\mu p^\mu$, and $x^2=-p_\mu n^\mu$. Given a master function $-\Lambda(n^2,p^2,x^2)$ (i.e., the superfluid analog of the equation of state), then the stress-energy tensor is

$$T^\mu_\nu=\Psi\delta^\mu_\nu+n^\mu\mu_\nu+p^\mu\chi_\nu, \tag{1}$$

where

$$\Psi=\Lambda-n^\rho\mu_\rho-p^\rho\chi_\rho \tag{2}$$

is the generalized pressure and

$$\mu_\nu=\mathcal{B}n_\nu+\mathcal{A}p_\nu, \quad \chi_\nu=\mathcal{A}n_\nu+\mathcal{C}p_\nu, \tag{3}$$

are the chemical potential covectors which also function as the respective momenta for the fluid elements. The $\mathcal{A}$, $\mathcal{B}$, and $\mathcal{C}$ coefficients are obtained from the master function via the partial derivatives

$$\mathcal{A}=-\frac{\partial\Lambda}{\partial x^2}, \quad \mathcal{B}=-2\frac{\partial\Lambda}{\partial n^2}, \quad \mathcal{C}=-2\frac{\partial\Lambda}{\partial p^2}. \tag{4}$$

The fact that the neutron momentum μ_μ, say, is not simply proportional to its number density current n^μ is a result of entrainment between the neutrons and protons, which we see vanishes if the $\mathcal{A}$ coefficient is zero.

Finally the equations for the neutrons and protons consist of the two conservation equations

$$\nabla_\mu n^\mu = 0, \quad \nabla_\mu p^\mu = 0, \tag{5}$$

and the two Euler equations

$$n^\mu \nabla_{[\mu} \mu_{\nu]} = 0, \quad p^\mu \nabla_{[\mu} \chi_{\nu]} = 0, \tag{6}$$

where the square braces mean antisymmetrization of the enclosed indices. Comer [30] and Prix *et al.* [12] discuss in some detail why the assumption of separate conservation for the two fluids should be reasonable for slow rotation and quasinormal mode calculations.

B. The slow-rotation expansions

Andersson and Comer [18] have adapted to the superfluid case the ordinary fluid slow rotation scheme originally developed by Hartle [31]. The configurations are assumed to be axisymmetric, asymptotically flat, and stationary, with the metric taking the form

$$g_{\mu\nu} dx^\mu dx^\nu = -(N^2 - \sin^2\theta K [N^\phi]^2) dt^2 + V dr^2 - 2 \sin^2\theta K N^\phi dt d\phi + K(d\theta^2 + \sin^2\theta d\phi^2). \tag{7}$$

The neutrons and protons are assumed to be rigidly rotating about the symmetry axis, with rates Ω_n and Ω_p, respectively, and unit four-velocities written as

$$u_n^\mu = \frac{t^\mu + \Omega_n \phi^\mu}{\sqrt{N^2 - \sin^2\theta K (N^\phi - \Omega_n)^2}},$$

$$u_p^\mu = \frac{t^\mu + \Omega_p \phi^\mu}{\sqrt{N^2 - \sin^2\theta K (N^\phi - \Omega_p)^2}}, \tag{8}$$

where t^μ is the Killing vector associated with the stationarity, and ϕ^μ with the axisymmetry.

The slow-rotation approximation assumes the rotation rates Ω_n and Ω_p are small in the sense that they should respect the inequalities (cf. [18,31])

$$\Omega_n^2 \text{ or } \Omega_p^2 \text{ or } \Omega_n \Omega_p \ll \left(\frac{c}{R}\right)^2 \frac{GM}{Rc^2}, \tag{9}$$

where the speed of light c and Newton's constant G have been restored, and M and R are the mass and radius, respectively, of the non-rotating configuration. Because $GM/c^2R < 1$, the inequalities naturally imply $\Omega_n R \ll c$ and $\Omega_p R \ll c$. The slow-rotation scheme has been shown, for instance in Prix *et al.* [12], to be a very good approximation for the fastest known pulsar, and starts to fail by about 15% to 20% for stars rotating at their Kepler limit.

In the same manner as Hartle, the metric is expanded like

$$N = e^{\nu(r)/2}(1 + h(r,\theta)),$$

$$V = e^{\lambda(r)}(1 + 2v(r,\theta)),$$

$$K = r^2(1 + 2k(r,\theta)),$$

$$N^\phi = \omega(r), \tag{10}$$

where ω is understood to be of $\mathcal{O}(\Omega_{n,p})$ and h, v, and k of $\mathcal{O}(\Omega_{n,p}^2)$. For later convenience we will also introduce

$$\tilde{L}_n = \omega - \Omega_n \text{ and } \tilde{L}_p = \omega - \Omega_p. \tag{11}$$

The expansion for the neutron and proton number densities n and p, respectively, are written as

$$n = n_o(r)(1 + \eta(r,\theta)), \quad p = p_o(r)(1 + \Phi(r,\theta)), \tag{12}$$

where the terms η and Φ are understood to be of $\mathcal{O}(\Omega_{n,p}^2)$ and we have introduced the convention that terms with an "o" subscript are either contributions from the non-rotating background or quantities that are evaluated on the non-rotating background (e.g. $x_o^2 = n_o p_o$ etc.). One can show furthermore that the metric corrections h, v, and k can be decomposed into "$l=0$" and "$l=2$" terms using Legendre polynomials for the angular dependence, i.e.,

$$h = h_0(r) + h_2(r) P_2(\cos\theta),$$

$$v = v_0(r) + v_2(r) P_2(\cos\theta),$$

$$k = k_2(r) P_2(\cos\theta), \tag{13}$$

where $P_2(\cos\theta) = (3\cos^2\theta - 1)/2$. As well we can write for the matter corrections

$$\eta = \eta_0(r) + \eta_2(r) P_2(\cos\theta), \quad \Phi = \Phi_0(r) + \Phi_2(r) P_2(\cos\theta). \tag{14}$$

Lastly, Andersson and Comer [18] have introduced a coordinate transformation $r \to r + \xi(r,\theta)$ that maps constant energy surfaces (i.e., the level surfaces of Λ_o) for the non-rotating background into the rotationally modified constant energy surfaces. The mapping ξ is given as

$$\mu_o n_o \eta_0 + \chi_o p_o \Phi_0 + \frac{r^2}{3e^\nu} \mathcal{A}_o n_o p_o (\Omega_n - \Omega_p)^2 = \Lambda_o' \xi_0 \tag{15}$$

for $l=0$ and for $l=2$

$$\mu_o n_o \eta_2 + \chi_o p_o \Phi_2 - \frac{r^2}{3e^\nu} \mathcal{A}_o n_o p_o (\Omega_n - \Omega_p)^2 = \Lambda_o' \xi_2, \tag{16}$$

where $\mu_o = \mathcal{B}_o n_o + \mathcal{A}_o p_o$ and $\chi_o = \mathcal{C}_o p_o + \mathcal{A}_o n_o$.

C. The slow-rotation equations

No different in number, but different in form from the ordinary fluid case considered by Hartle, the Einstein and superfluid field equations reduce to four sets: (i) the nonrotating background that determines ν, λ, n_o, and p_o, (ii) the linear order that calculates the "frame-dragging" ω, (iii) the $l=0$ second order equations that yield ξ_0, η_0, Φ_0, h_0, and v_0, and (iv) the $l=2$ set at second order that determines ξ_2, η_2, Φ_2, h_2, v_2, and k_2. For convenience we list the equa-

tions here and recall where appropriate the free parameters of the system and how they are specified during a numerical integration.

1. The $\mathcal{O}=(\Omega^0_{n,p})$ or background equations

The background equations are

$$\lambda' = \frac{1-e^{\lambda}}{r} - 8\pi r e^{\lambda}\Lambda_{\rm o}, \tag{17}$$

$$\nu' = -\frac{1-e^{\lambda}}{r} + 8\pi r e^{\lambda}\Psi_{\rm o}, \tag{18}$$

$$0 = \mathcal{A}^0_0|_{\rm o} p_{\rm o}' + \mathcal{B}^0_0|_{\rm o} n_{\rm o}' + \frac{1}{2}\mu_{\rm o}\nu', \tag{19}$$

$$0 = \mathcal{C}^0_0|_{\rm o} p_{\rm o}' + \mathcal{A}^0_0|_{\rm o} n_{\rm o}' + \frac{1}{2}\chi_{\rm o}\nu', \tag{20}$$

where the $\mathcal{A}^0_0|_{\rm o}$, $\mathcal{B}^0_0|_{\rm o}$, and $\mathcal{C}^0_0|_{\rm o}$ coefficients are obtained from the master function and will be discussed in much greater detail below (cf. Secs. II D, III, and the Appendix). Throughout a prime "′" will denote differentiation with respect to r.

Regularity at the origin implies that $\lambda(0)$, $\lambda'(0)$, $\nu'(0)$, $n_{\rm o}'(0)$, and $p_{\rm o}'(0)$ all vanish. The radius R is obtained from the condition that the pressure vanish on the surface [i.e., $\Psi_{\rm o}(R)=0$] and the background mass is given by

$$M = -4\pi\int_0^R \Lambda_{\rm o}(r) r^2 {\rm d}r. \tag{21}$$

The parameters $n_{\rm o}(0)$ and $p_{\rm o}(0)$ for the matter on the background are not independent because chemical equilibrium is imposed between the neutrons, protons, and a highly degenerate gas of relativistic electrons (cf. the Appendix).

2. The $\mathcal{O}(\Omega_{n,p})$ or frame-dragging equation

For $\mathcal{O}(\Omega_{n,p})$ there is only the frame-dragging $\omega(r)$, which is determined from

$$\frac{1}{r^4}(r^4 e^{-(\lambda+\nu)/2}\tilde{L}_n')' - 16\pi e^{(\lambda-\nu)/2}(\Psi_{\rm o}-\Lambda_{\rm o})\tilde{L}_n = 16\pi e^{(\lambda-\nu)/2}\chi_{\rm o} p_{\rm o}(\Omega_n-\Omega_p). \tag{22}$$

The key difference with the frame-dragging equation for an ordinary fluid is the "source" term on the right-hand side. Any solution must be such that it joins smoothly to the exterior vacuum solution. Continuity implies that

$$\tilde{L}_n(R) = -\Omega_n + \frac{2J}{R^3}, \tag{23}$$

where J is the total angular momentum of the system. Using also that the derivative at the surface is to be continuous implies

$$\tilde{L}_n(R) = -\Omega_n - \frac{R}{3}\tilde{L}_n'(R). \tag{24}$$

When the frame-dragging equation is solved numerically, one searches for a central value $\tilde{L}_n(0)$ that allows Eq. (24) to be satisfied.

With a solution in hand, the neutron and proton angular momenta, J_n and J_p, respectively, can then be calculated using

$$J_n = -\frac{8\pi}{3}\int_0^R {\rm d}r r^4 e^{(\lambda-\nu)/2}[\mu_{\rm o} n_{\rm o}\tilde{L}_n + \mathcal{A}_{\rm o} n_{\rm o} p_{\rm o}(\Omega_n-\Omega_p)] \tag{25}$$

and

$$J_p = -\frac{8\pi}{3}\int_0^R {\rm d}r r^4 e^{(\lambda-\nu)/2}[\chi_{\rm o} p_{\rm o}\tilde{L}_p + \mathcal{A}_{\rm o} n_{\rm o} p_{\rm o}(\Omega_p-\Omega_n)]. \tag{26}$$

The total angular momentum J likewise follows since $J = J_n + J_p$.

3. The $\mathcal{O}(\Omega^2_{n,p})$ equations

One should first note that at this order there will exist both a $l=0$ and $l=2$ set of equations. The $\mathcal{O}(\Omega^2_{n,p})$, $l=0$ set consists of Eq. (15) as well as

$$\gamma_n = \frac{\mathcal{B}^0_0|_{\rm o} n_{\rm o}}{\mu_{\rm o}}\eta_0 + \frac{\mathcal{A}^0_0|_{\rm o} p_{\rm o}}{\mu_{\rm o}}\Phi_0 + \frac{r^2}{3e^{\nu}}\frac{p_{\rm o}}{\mu_{\rm o}} \times\left(\mathcal{A}_{\rm o} + n_{\rm o}\frac{\partial\mathcal{A}}{\partial n}\bigg|_{\rm o} + n_{\rm o} p_{\rm o}\frac{\partial\mathcal{A}}{\partial x^2}\bigg|_{\rm o}\right)(\Omega_n-\Omega_p)^2 - \frac{r^2}{3e^{\nu}}\tilde{L}_n^2 + h_0, \tag{27}$$

$$\gamma_p = \frac{\mathcal{C}^0_0|_{\rm o} p_{\rm o}}{\chi_{\rm o}}\Phi_0 + \frac{\mathcal{A}^0_0|_{\rm o} n_{\rm o}}{\chi_{\rm o}}\eta_0 + \frac{r^2}{3e^{\nu}}\frac{n_{\rm o}}{\chi_{\rm o}} \times\left(\mathcal{A}_{\rm o} + p_{\rm o}\frac{\partial\mathcal{A}}{\partial p}\bigg|_{\rm o} + n_{\rm o} p_{\rm o}\frac{\partial\mathcal{A}}{\partial x^2}\bigg|_{\rm o}\right)(\Omega_n-\Omega_p)^2 - \frac{r^2}{3e^{\nu}}\tilde{L}_p^2 + h_0, \tag{28}$$

$$0 = \frac{16\pi r^2}{3e^{\nu}}[(\Psi_{\rm o}-\Lambda_{\rm o})\tilde{L}_n^2 + \chi_{\rm o} p_{\rm o}(\Omega_n-\Omega_p)(\tilde{L}_n+\tilde{L}_p) - \mathcal{A}_{\rm o} n_{\rm o} p_{\rm o}(\Omega_n-\Omega_p)^2] + 8\pi\Lambda_{\rm o}'\xi_0 - \frac{2}{r^2}\left(\frac{r}{e^{\lambda}}v_0\right)' + \frac{r^2}{6e^{\nu+\lambda}}(\tilde{L}_n')^2, \tag{29}$$

$$0=\frac{2}{re^{\lambda}}h_0'-\frac{2}{re^{\lambda}}\left(\nu'+\frac{1}{r}\right)v_0+\frac{r^2}{6e^{\nu+\lambda}}(\tilde{L}_n')^2-8\pi \times\left[\mu_o n_o\gamma_n+\chi_o p_o\gamma_p-(\Psi_o-\Lambda_o)h_0+\frac{r^2}{3e^{\nu}} \times(\mu_o n_o\tilde{L}_n^2+\chi_o p_o\tilde{L}_p^2)-\frac{r^2}{3e^{\nu}}n_o p_o\mathcal{A}_o(\Omega_n-\Omega_p)^2\right]. \tag{30}$$

Here γ_n and γ_p are integration constants, which are determined from data given at the center of the star:

$$\gamma_n=h_0(0)+\left(\frac{\mu_o\mathcal{A}_0^0|_o-\chi_o\mathcal{B}_0^0|_o}{\mu_o^2}p_o\Phi_0\right)\Bigg|_{r=0}, \tag{31}$$

$$\gamma_p=h_0(0)+\left(\frac{\mu_o\mathcal{C}_0^0|_o-\chi_o\mathcal{A}_0^0|_o}{\mu_o\chi_o}p_o\Phi_0\right)\Bigg|_{r=0}. \tag{32}$$

It is convenient to define the new variable $m_0=rv_0/\exp(\lambda)$. Because we must have $\xi_0(0)=0$, then $\eta_0(0)$ and $\Phi_0(0)$ are related via

$$(\mu_o n_o\eta_0)|_{r=0}+(\chi_o p_o\Phi_0)|_{r=0}=0. \tag{33}$$

Regularity at the center of the star also requires that $m_0(0)=0$, but $h_0(0)$ and $\eta_0(0)$, say, are freely specified.

As for the $\mathcal{O}(\Omega_{n,p}^2)$, $l=2$ equations, in addition to Eq. (16), we have

$$0=\frac{\mathcal{B}_0^0|_o n_o}{\mu_o}\eta_2+\frac{\mathcal{A}_0^0|_o p_o}{\mu_o}\Phi_2-\frac{r^2}{3e^{\nu}}\frac{p_o}{\mu_o} \times\left(\mathcal{A}_o+n_o\frac{\partial\mathcal{A}}{\partial n}\Big|_o+n_o p_o\frac{\partial\mathcal{A}}{\partial x^2}\Big|_o\right)(\Omega_n-\Omega_p)^2 +\frac{r^2}{3e^{\nu}}\tilde{L}_n^2+h_2, \tag{34}$$

$$0=\frac{\mathcal{C}_0^0|_o p_o}{\chi_o}\Phi_2+\frac{\mathcal{A}_0^0|_o n_o}{\chi_o}\eta_2-\frac{r^2}{3e^{\nu}}\frac{n_o}{\chi_o} \times\left(\mathcal{A}_o+p_o\frac{\partial\mathcal{A}}{\partial p}\Big|_o+n_o p_o\frac{\partial\mathcal{A}}{\partial x^2}\Big|_o\right)(\Omega_n-\Omega_p)^2 +\frac{r^2}{3e^{\nu}}\tilde{L}_p^2+h_2, \tag{35}$$

$$v_2+h_2=\frac{r^4}{6e^{\nu+\lambda}}(\tilde{L}_n')^2+\frac{8\pi r^4}{3e^{\nu}}(\Psi_o-\Lambda_o)\tilde{L}_n^2 +\frac{8\pi r^4}{3e^{\nu}}[\chi_o p_o(\Omega_n-\Omega_p)(\tilde{L}_n+\tilde{L}_p) -\mathcal{A}_o n_o p_o(\Omega_n-\Omega_p)^2], \tag{36}$$

$$0=\frac{1}{r}(v_2+h_2)-(k_2+h_2)'-\frac{\nu'}{2}(h_2-v_2), \tag{37}$$

$$0=\frac{2}{re^{\lambda}}h_2'-\frac{6}{r^2}h_2-\frac{2}{re^{\lambda}}\left(\nu'+\frac{1}{r}\right)v_2 +\frac{1}{e^{\lambda}}\left(\nu'+\frac{2}{r}\right)k_2'-\frac{4}{r^2}k_2-\frac{r^2}{6e^{\nu+\lambda}}(\tilde{L}_n')^2 +8\pi\left[(\Psi_o-\Lambda_o)h_2+\frac{r^2}{3e^{\nu}}(\mu_o n_o\tilde{L}_n^2+\chi_o p_o\tilde{L}_p^2) -\frac{r^2}{3e^{\nu}}n_o p_o\mathcal{A}_o(\Omega_n-\Omega_p)^2\right]. \tag{38}$$

In contrast to the $l=0$ case, the condition that $\xi_2(0)=0$ at the center of the star leads to $\eta_2(0)=0=\Phi_2(0)$. Also note that Eq. (36) can be used to remove v_2 in terms of the functions h_2 and $\tilde{L}_{n,p}$. It is furthermore convenient to work with the new variable $\tilde{k}=h_2+k_2$ [31]. Regularity at the center of the star implies that $h_2(r)\sim c_1 r^2$ and $\tilde{k}(r)\sim c_2 r^4$ as $r\to 0$, where the constants c_1 and c_2 are related by

$$c_1+2\pi\left(\Psi_o(0)-\frac{1}{3}\Lambda_o(0)\right)c_2=0. \tag{39}$$

We can take advantage of an overall scale invariance of the field equations to remove the explicit dependence on both Ω_n and Ω_p by dividing through by Ω_p, the net result being that only the ratio Ω_n/Ω_p needs to be specified in advance. As for the other parameters, they are chosen so that the solutions obtained join smoothly to a vacuum exterior. For $l=0$, after Ω_n/Ω_p and $\eta_0(0)$ are specified, this means a search over $h_0(0)$ is performed until a smooth solution is achieved. For $l=2$, the situation is slightly more involved, requiring that homogeneous and then particular solutions be obtained for the set $(h_2,\tilde{k})$ (see [18] for more details). By searching over c_1, say, and also trying different linear combinations of homogeneous and particular solutions eventually smoothness with the vacuum exterior can be achieved.

Having obtained a complete solution, the rotationally induced change to the mass can be determined using

$$\delta M=(R-2M)v_0(R)+\frac{J^2}{R^3}. \tag{40}$$

Also the rotationally induced changes to the neutron and proton particle numbers are obtained, respectively, from

$$\delta N_n = \int_0^R dr r^2 e^{\lambda/2} n_o \left(\eta_0 + v_0 + \left[\frac{\lambda'}{2} + \frac{2}{r} \right] \xi_0 + \frac{2r^2}{3e^\nu} \tilde{L}_n^2 \right) \quad (41)$$

and

$$\delta N_p = \int_0^R dr r^2 e^{\lambda/2} p_o \left(\Phi_0 + v_0 + \left[\frac{\lambda'}{2} + \frac{2}{r} \right] \xi_0 + \frac{2r^2}{3e^\nu} \tilde{L}_p^2 \right). \quad (42)$$

Finally, the Kepler frequency Ω_K is calculated (cf. [32] and [18]) using the slow-rotation form of

$$\Omega_K = \frac{Nv}{\sqrt{K}} + \omega, \quad (43)$$

where the metric variables are those of Eq. (7) and

$$v = \frac{K^{3/2}\omega'}{NK'} + \sqrt{\frac{2KN'}{NK'} + \left(\frac{K^{3/2}\omega'}{NK'} \right)^2} \quad (44)$$

is the orbital velocity according to a zero-angular momentum observer at the equator (where all quantities are to be evaluated). In the slow rotation approximation, the Kepler limit is the solution to

$$\Omega_K = \sqrt{\frac{M}{R^3}} - \frac{\hat{J}\Omega_p}{R^3} + \sqrt{\frac{M}{R}} \left\{ \frac{\delta \hat{M}}{2M} + \frac{(R+3M)(3R-2M)}{4R^4M^2} \hat{J}^2 - \frac{3}{4} \frac{2\hat{\xi}_0 + \hat{\xi}_2}{R^2} + \alpha \hat{A} \right\} \Omega_p^2, \quad (45)$$

where we have made the scaling with Ω_p explicit by introducing $J = \hat{J}\Omega_p$, etc., and have also defined

$$\alpha = \frac{3(R^3 - 2M^3)}{4M^3} \log\left(1 - \frac{2M}{R} \right) + \frac{3R^4 - 3R^3M - 2R^2M^2 - 8RM^3 + 6M^4}{2RM^2(R-2M)}. \quad (46)$$

In solving Eq. (45) we fix first the ratio Ω_n/Ω_p. If $|\Omega_n/\Omega_p| < 1$, then we insert $\Omega_K = \Omega_p$ and solve for Ω_p, otherwise we set $\Omega_K = (\Omega_n/\Omega_p)\Omega_p$ and then again solve for Ω_p.

D. Analytic expansion for the local matter content

Before proceeding to the next section that describes the mean field approach, one final observation needs to be made. We see in the equations above the appearance of not only the entrainment, via the $\mathcal{A}$ coefficient, but also the relative velocity-dependent part of the entrainment, through the term $\partial\mathcal{A}/\partial x^2$. *A priori* one needs a formalism for the matter that will determine this term, if the effects of a relative rotation between the neutrons and protons are to be consistently incorporated. The mean field formalism presented in Sec. III can do just that. However, before embarking on a full-fledged calculation, it is very worthwhile to consider next the implications of the slow rotation expansion for the master function.

The term $\partial\mathcal{A}/\partial x^2$ would seem to imply, at least in principle, that we need to know the master function to $\mathcal{O}(x^4)$. Consider, then, regions of the matter (i.e., fluid elements) that are local enough that their spacetime can be taken to be that of Minkowski, so that we can write out the x^2 term explicitly as

$$x^2 = np \left(\frac{1 - \vec{v}_n \cdot \vec{v}_p/c^2}{\sqrt{1-(v_n/c)^2}\sqrt{1-(v_p/c)^2}} \right), \quad (47)$$

where $\vec{v}_n$ and $\vec{v}_p$ are the neutron and proton, respectively, three-velocities in the local Minkowski frame. We see from this that when the individual three-velocities $\vec{v}_{n,p}$ satisfy $v_{n,p}/c \ll 1$, then $x^2 \approx np$ to leading order in the ratios v_n/c and v_p/c.

With this as motivation we write an analytic expansion for the master function of the form [8,13]

$$\Lambda(n^2, p^2, x^2) = \sum_{i=0}^{\infty} \lambda_i(n^2, p^2)(x^2 - np)^i. \quad (48)$$

The $\mathcal{A}$, $\mathcal{A}_0^0$, etc. coefficients that appear in the field equations can now be written as

$$\mathcal{A} = -\lambda_1 - \sum_{i=2}^{\infty} i\lambda_i (x^2 - np)^{i-1}, \quad (49)$$

$$\mathcal{B} = -\frac{1}{n}\frac{\partial \lambda_0}{\partial n} - \frac{p}{n}\mathcal{A} - \frac{1}{n}\sum_{i=1}^{\infty} \frac{\partial \lambda_i}{\partial n}(x^2 - np)^i, \quad (50)$$

$$\mathcal{C} = -\frac{1}{p}\frac{\partial \lambda_0}{\partial p} - \frac{n}{p}\mathcal{A} - \frac{1}{p}\sum_{i=1}^{\infty} \frac{\partial \lambda_i}{\partial p}(x^2 - np)^i, \quad (51)$$

$$\mathcal{A}_0^0 = -\frac{\partial^2 \lambda_0}{\partial p \partial n} - \sum_{i=1}^{\infty} \frac{\partial^2 \lambda_i}{\partial p \partial n}(x^2 - np)^i, \quad (52)$$

$$\mathcal{B}_0^0 = -\frac{\partial^2 \lambda_0}{\partial n^2} - \sum_{i=1}^{\infty} \frac{\partial^2 \lambda_i}{\partial n^2}(x^2 - np)^i, \quad (53)$$

$$\mathcal{C}_0^0 = -\frac{\partial^2 \lambda_0}{\partial p^2} - \sum_{i=1}^{\infty} \frac{\partial^2 \lambda_i}{\partial p^2}(x^2 - np)^i, \quad (54)$$

$$\frac{\partial \mathcal{A}}{\partial n} = -\frac{\partial \lambda_1}{\partial n} - \sum_{i=2}^{\infty} i \left(\frac{\partial \lambda_i}{\partial n}[x^2 - np] - [i-1]p\lambda_i \right) \times (x^2 - np)^{i-2}, \quad (55)$$

$$\frac{\partial \mathcal{A}}{\partial p} = -\frac{\partial \lambda_1}{\partial p} - \sum_{i=2}^{\infty} i \left(\frac{\partial \lambda_i}{\partial p}[x^2 - np] - [i-1]n\lambda_i \right) \times (x^2 - np)^{i-2}, \quad (56)$$

$$\frac{\partial \mathcal{A}}{\partial x^2} = -2\lambda_2 - \sum_{i=3}^{\infty} i(i-1)\lambda_i (x^2 - np)^{i-2}. \tag{57}$$

We conclude from this expansion that the master function coefficients λ_0, λ_1, and λ_2 uniquely determine the background values for all the matter coefficients—i.e., $\mathcal{A}_o$, $\mathcal{B}_o$, etc.—that enter the field equations. In particular, if we need to know λ_2 then we need to know the master function to at least $\mathcal{O}(x^4)$. However, the particular combinations that contain $\partial\mathcal{A}/\partial x^2$ that enter the field equations are seen to reduce to

$$\mathcal{A} + n\frac{\partial \mathcal{A}}{\partial n} + np\frac{\partial \mathcal{A}}{\partial x^2} = -\lambda_1 - n\frac{\partial \lambda_1}{\partial n} - \sum_{i=2}^{\infty} \left(\lambda_i + n\frac{\partial \lambda_i}{\partial n}\right)(x^2 - np)^{i-1}, \tag{58}$$

$$\mathcal{A} + p\frac{\partial \mathcal{A}}{\partial p} + np\frac{\partial \mathcal{A}}{\partial x^2} = -\lambda_1 - p\frac{\partial \lambda_1}{\partial p} - \sum_{i=2}^{\infty} \left(\lambda_i + p\frac{\partial \lambda_i}{\partial p}\right)(x^2 - np)^{i-1}. \tag{59}$$

That is, these combinations involve only the λ_1 coefficient when evaluated on the background. This, in fact, makes perfect sense since the slow rotation approximation is to $\mathcal{O}(\Omega_{n,p}^2)$, which naturally corresponds to the term in the master function proportional to $x^2 - np$.

III. THE σ-ω RELATIVISTIC MEAN FIELD MODEL

The master function to be used has been obtained using a relativistic σ-ω mean field model of the type described by Glendenning [16]. The Lagrangian for this system is given by

$$L = L_b + L_\sigma + L_\omega + L_{int}, \tag{60}$$

where

$$L_b = \bar{\psi}(i\gamma_\mu \partial^\mu - m)\psi, \tag{61}$$

$$L_\sigma = -\frac{1}{2}\partial_\mu \sigma \partial^\mu \sigma - \frac{1}{2}m_\sigma^2 \sigma^2, \tag{62}$$

$$L_\omega = -\frac{1}{4}\omega_{\mu\nu}\omega^{\mu\nu} - \frac{1}{2}m_\omega^2 \omega_\mu \omega^\mu, \tag{63}$$

$$L_{int} = g_\sigma \sigma \bar{\psi}\psi - g_\omega \omega_\mu \bar{\psi}\gamma^\mu \psi. \tag{64}$$

Here m is the baryon mass, ψ is an 8-component spinor with the proton components as the top 4 and the neutron components as the bottom 4, the γ_μ are the corresponding 8×8 block diagonal Dirac matrices, and $\omega_{\mu\nu} = \partial_\mu \omega_\nu - \partial_\nu \omega_\mu$. The coupled set of field equations obtained from this Lagrangian

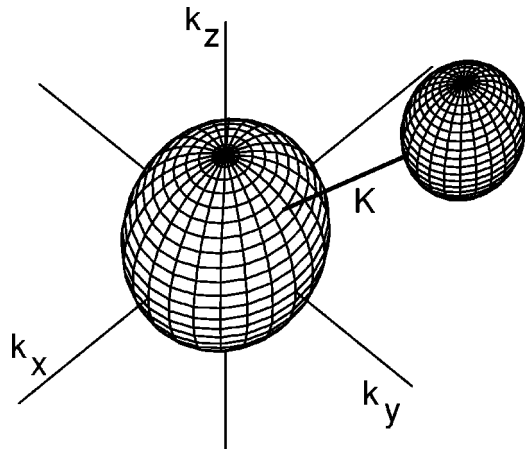

FIG. 1. The neutron and proton Fermi spheres drawn in momentum space. The neutron sphere is centered at the origin and has radius k_n, whereas the proton sphere has radius k_p and its center has been displaced an amount K from the origin.

are to be solved in each fluid element of the neutron star. The main approximations of the mean field approach are to assume that the nucleons can be represented as plane-wave states and that all gradients of the σ and ω^μ fields can be ignored. The coupling constants g_σ and g_ω and field masses m_σ and m_ω are determined, for instance, from properties of nuclear matter at the nuclear saturation density. Fortunately, in what follows, we only need to give the ratios $c_\sigma^2 = (g_\sigma/m_\sigma)^2$ and $c_\omega^2 = (g_\omega/m_\omega)^2$.

Of course, the main consideration is to produce a master function that incorporates the entrainment effect. Consider again fluid elements somewhere in the neutron star. The fermionic nature of the nucleons means that they are to be placed into the various energy levels (obtained from the mean field calculation) until their respective (local) Fermi spheres are filled. The Fermi spheres are best visualized in momentum space, as in Fig. 1. The entrainment is incorporated by displacing the center of the proton Fermi sphere from that of the neutron Fermi sphere, also illustrated in Fig. 1. The neutron sphere is centered on the origin, and has a radius k_n. Displaced an amount K from the origin is the center of the proton sphere, which has a radius k_p. The Fermi sphere radii and displacement (k_n, k_p, K) are functions of the local neutron and proton number densities and the local, relative velocity of the protons, say, with respect to the neutrons.

Introducing the definitions

$$\phi_n \equiv g_\omega \omega^z, \quad \phi_p \equiv \phi_n + K, \tag{65}$$

then the master function takes the form [8]

$$\Lambda = -\frac{c_\omega^2}{18\pi^4}(k_n^3 + k_p^3)^2 + \frac{1}{2c_\omega^2}\phi_n^2 - \frac{1}{2c_\sigma^2}(m^2 - m_*^2) - 3\langle \bar{\Psi}\gamma^x k_x \Psi\rangle, \tag{66}$$

where

$$\langle\overline{\Psi}\gamma^x k_x\Psi\rangle=\frac{1}{12\pi^2}\Bigg(\int_{-k_n}^{k_n}dk_z[(k_n^2-2m_*^2-2\phi_n^2-3k_z^2-4\phi_n k_z)(k_n^2+\phi_n^2+m_*^2+2\phi_n k_z)^{1/2}+2([k_z+\phi_n]^2+m_*^2)^{3/2}]+\int_{-k_p}^{k_p}dk_z[(k_p^2-2m_*^2-2\phi_p^2-3k_z^2-4\phi_p k_z)(k_p^2+\phi_p^2+m_*^2+2\phi_p k_z)^{1/2}+2([k_z+\phi_p]^2+m_*^2)^{3/2}]\Bigg),\tag{67}$$

$$m_*=m-\frac{c_\sigma^2}{2\pi^2}m_*\Bigg(\int_{-k_n}^{k_n}dk_z[k_n^2+\phi_n^2+m_*^2+2\phi_n k_z]^{1/2}+\int_{-k_p}^{k_p}dk_z[k_p^2+\phi_p^2+m_*^2+2\phi_p k_z]^{1/2}-\int_{-k_n}^{k_n}dk_z[(k_z+\phi_n)^2+m_*^2]^{1/2}-\int_{-k_p}^{k_p}dk_z[(k_z+\phi_p)^2+m_*^2]^{1/2}\Bigg),\tag{68}$$

$$n^0=\frac{1}{3\pi^2}k_n^3,\tag{69}$$

$$p^0=\frac{1}{3\pi^2}k_p^3,\tag{70}$$

$$n^z=\frac{1}{2\pi^2}\int_{-k_n}^{k_n}dk_z(k_z+\phi_n)([k_n^2+m_*^2+\phi_n^2+2\phi_n k_z]^{1/2}-[(k_z+\phi_n)^2+m_*^2]^{1/2}),\tag{71}$$

$$p^z=\frac{1}{2\pi^2}\int_{-k_p}^{k_p}dk_z(k_z+\phi_p)([k_p^2+m_*^2+\phi_p^2+2\phi_p k_z]^{1/2}-[(k_z+\phi_p)^2+m_*^2]^{1/2}),\tag{72}$$

$$\phi_n=-c_\omega^2(n^z+p^z).\tag{73}$$

As applied to this system, the slow-rotation approximation means that K is small with respect to $k_{n,p}$. In particular, we should keep terms up to and including $\mathcal{O}(K^2)$.

Implementation of the mean-field approach is hampered by the fact that the most natural variables for it are the momenta (k_n,k_p,K), whereas the general relativistic superfluid formalism relies on (n^2,p^2,x^2). The two sets are related to each other via the kinematic relations

$$n^2=(n^0)^2-(n^z)^2,\quad p^2=(p^0)^2-(p^z)^2,\quad x^2=n^0p^0-n^zp^z,\tag{74}$$

where n^0, p^0, n^z, and p^z are given above in Eqs. (69), (70), (71), and (72). In principle one would specify values for the set (n^2,p^2,x^2), and then use Eqs. (69), (70), (71), and (72) in Eq. (74) to determine the set (k_n,k_p,K). One would then solve Eq. (68) for the Dirac effective mass m_*. In practice we rewrite the field equations so as to solve directly for (k_n,k_p,K).

TABLE I. The canonical background models used here and by Comer and Joynt [8].

Model I	Model II
$(g_\sigma/m_\sigma)^2=12.684$	$(g_\sigma/m_\sigma)^2=8.403$
$(g_\omega/m_\omega)^2=7.148$	$(g_\omega/m_\omega)^2=4.233$
$\nu(0)=-2.316408$	$\nu(0)=-2.288385$
$k_n(0)=2.8\ \mathrm{fm}^{-1}$	$k_n(0)=3.25\ \mathrm{fm}^{-1}$
$x_p(0)=0.101$	$x_p(0)=0.102$
$M=2.509M_\odot$	$M=1.996M_\odot$
$R=11.696$ km	$R=9.432$ km
$\eta_0(0)=0$	$\eta_0(0)=0$

Earlier we discussed the slow-rotation approximation as it applies to the master function, and determined that we need to know the λ_0 and λ_1 coefficients. Comer and Joynt [8] have shown that

$$\lambda_0=-\frac{c_\omega^2}{18\pi^4}(k_n^3+k_p^3)^2-\frac{1}{4\pi^2}(k_n^3\sqrt{k_n^2+m_*|_o^2}+k_p^3\sqrt{k_p^2+m_*|_o^2})-\frac{1}{4c_\sigma^2}(2m-m_*|_o)(m-m_*|_o)-\frac{1}{8\pi^2}\Bigg(m_e k_p[2k_p+m_e]\sqrt{k_p^2+m_e^2}-m_e^4\ln\left[\frac{k_p+\sqrt{k_p^2+m_e^2}}{m_e}\right]\Bigg),\tag{75}$$

$$\lambda_1=-c_\omega^2-\frac{c_\omega^2}{5\mu_o^2}\Bigg(2k_p^2\frac{\sqrt{k_n^2+m_*|_o^2}}{\sqrt{k_p^2+m_*|_o^2}}+\frac{c_\omega^2}{3\pi^2}\times\left[\frac{k_n^2k_p^3}{\sqrt{k_n^2+m_*|_o^2}}+\frac{k_p^2k_n^3}{\sqrt{k_p^2+m_*|_o^2}}\right]\Bigg)-\frac{3\pi^2k_p^2}{5\mu_o^2k_n^3}\frac{k_n^2+m_*|_o^2}{\sqrt{k_p^2+m_*|_o^2}},\tag{76}$$

where $m_*|_o$ is the solution to the transcendental equation

$$m_*|_o=m-m_*|_o\frac{c_\sigma^2}{2\pi^2}\Bigg(k_n\sqrt{k_n^2+m_*|_o^2}+k_p\sqrt{k_p^2+m_*|_o^2}-\frac{1}{2}m_*\Big|_o^2\ln\left[\frac{k_n+\sqrt{k_n^2+m_*|_o^2}}{-k_n+\sqrt{k_n^2+m_*|_o^2}}\right]-\frac{1}{2}m_*\Big|_o^2\ln\left[\frac{k_p+\sqrt{k_p^2+m_*|_o^2}}{-k_p+\sqrt{k_p0^2+m_*|_o^2}}\right]\Bigg)\tag{77}$$

and we have added to λ_0 the contributions due to the electrons ($m_e=m/1836$). This is necessary to obtain a central

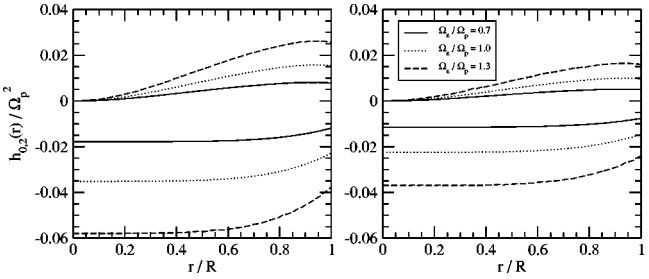

FIG. 2. The metric functions $h_0(r)$—the 3 lower curves—and $h_2(r)$—the 3 upper curves—vs r for models I (left panel) and II (right panel) of Table I. The relative rotation rates are varied ($\Omega_n/\Omega_p = 0.7,\ 1.0,\ 1.3$).

proton fraction $p_o(0)/(p_o(0)+n_o(0))$ of about 0.1, which is considered typical for neutron stars.

In order to solve for the background, we note that

$$n_o = \frac{k_n^3}{3\pi^2}, \quad p_o = \frac{k_p^3}{3\pi^2}. \tag{78}$$

That is, we replace everywhere the background neutron and proton number densities with their respective Fermi momenta. Once the Fermi momenta are specified, we can then determine the background value for the Dirac effective mass, i.e. $m_*|_o$, from Eq. (77). However, Comer and Joynt found that numerical solutions were easier to obtain by turning Eq. (77) into a differential equation using the identity

$$m_*|_o{}' = \frac{\partial m_*|_o}{\partial k_n} k_n' + \frac{\partial m_*|_o}{\partial k_p} k_p', \tag{79}$$

and where k_n' and k_p' are to be obtained simultaneously using Eq. (20). The partial derivatives of the Dirac effective mass can be found in the Appendix, along with the other matter coefficients.

IV. NUMERICAL RESULTS

In this section we present numerical solutions to the slow rotation equations. The two canonical background configurations (see Table I) that will be used repeatedly are the same as those used by Comer and Joynt [8]. They are such that the neutron and proton number densities vanish on the same surface. They are also such that chemical equilibrium has been

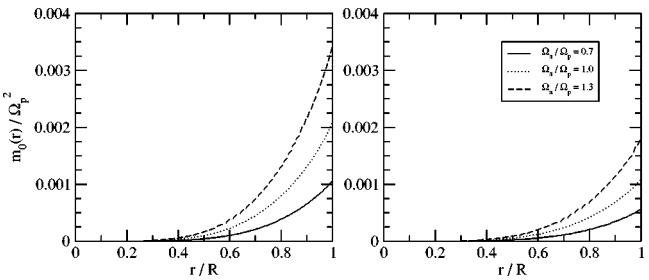

FIG. 3. The metric function $m_0(r) = r v_0(r)/\exp(\lambda(r))$ vs r for models I (left panel) and II (right panel) of Table I. The relative rotation rates are varied ($\Omega_n/\Omega_p = 0.7,\ 1.0,\ 1.3$).

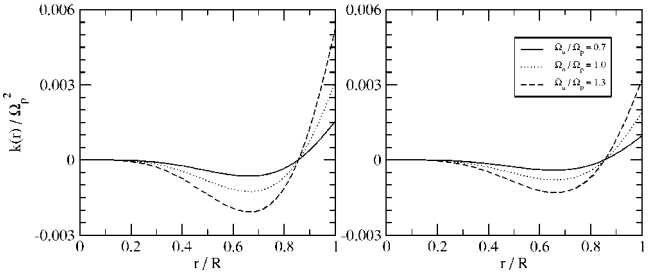

FIG. 4. The combination $\tilde{k}(r) = h_2(r) + k_2(r)$ vs r for models I (left panel) and II (right panel) of Table I. The relative rotation rates are varied ($\Omega_n/\Omega_p = 0.7,\ 1.0,\ 1.3$).

imposed, which implies that the proton number density at the center of the star is no longer a free parameter. We do not apply chemical equilibrium for the rotating configurations since Andersson and Comer [18] have shown it is not consistent with rigid rotation. The two sets of parameter values for the mean field model given in Table I represent the two extremes discussed by Glendenning [16]. For all of the solutions we will set $\eta_0(0) = 0$ which implies also that $\Phi_0(0) = 0$.

To begin we will give plots of the various field radial profiles for varying relative rotation rates of $\Omega_n/\Omega_p = 0.7, 1.0, 1.3$. These fall within the range of rates that were considered earlier by Comer and Joynt [8], who determined the frame-dragging and the angular momenta (cf. their Figs. 4 and 5). Picking up at the second order, we present in Fig. 2 a plot of $h_0(r)$ vs r for several relative rotation rates and for models I (left panel) and II (right panel) of Table I. Similarly in Fig. 3 we show a plot of $m_0(r) = r v_0(r)/\exp(\lambda(r))$ vs r and in Fig. 4 we have $\tilde{k}(r) = h_2(r) + k_2(r)$ vs r. Figure 5 shows the radial profiles of $\xi_0(r)$ and $\xi_2(r)$. Figures 6 and 7 show the radial profiles of $\eta_0(r)$ and $\eta_2(r)$ and $\Phi_0(r)$ and $\Phi_2(r)$, respectively. [We do not show plots of $v_2(r)$ since it can be removed in terms of $h_2(r)$ and $\tilde{L}_{n,p}(r)$.]

Andersson and Comer [18] used a simplified equation of state (i.e. a sum of polytropes) and did not include entrainment and thus a direct comparison between our solutions and theirs would not be expected to yield the same details. That being said, there are some qualitative similarities. For instance, the signs of the $l = 0$ fields versus the $l = 2$ fields are

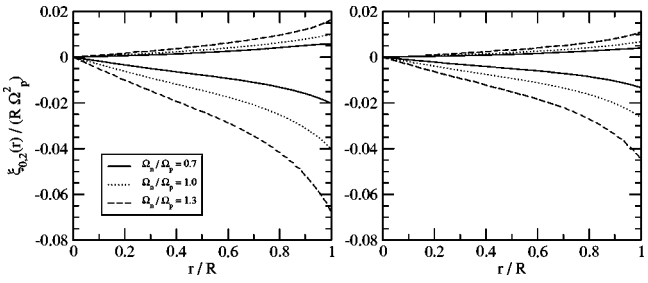

FIG. 5. The radial displacements $\xi_0(r)$—the 3 upper curves—and $\xi_2(r)$—the 3 lower curves—vs r for models I (left panel) and II (right panel) of Table I. The relative rotation rates are varied ($\Omega_n/\Omega_p = 0.7,\ 1.0,\ 1.3$).

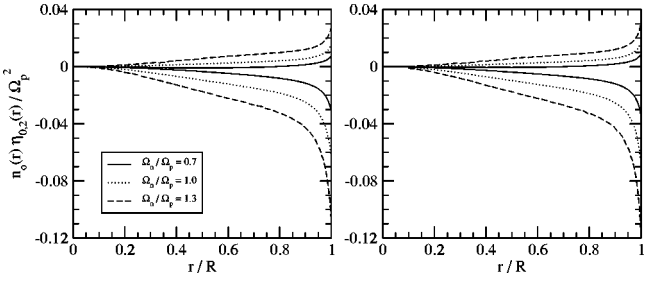

FIG. 6. The neutron density corrections $n_o(r)\,\eta_0(r)$—the 3 upper curves—and $n_o(r)\,\eta_2(r)$—the 3 lower curves—vs r for models I (left panel) and II (right panel) of Table I. The relative rotation rates are varied ($\Omega_n/\Omega_p = 0.7,\ 1.0,\ 1.3$).

in agreement, as are the number of zeroes that occur in the fields. The most pronounced qualitative differences are found in the functions $\Phi_0(r)$ and $\Phi_2(r)$, especially near the surface of the star. This could perhaps be related to our use of an explicit term for the electrons in the equation of state.

In Fig. 8 we have graphed the total mass for proton rotation rates that equal the fastest known pulsar (i.e., $\Omega_p = 3900$ rad/s) versus the background central neutron number density. The left panel is for model I of Table I and the right panel is for model II. In both plots the relative rotation rate Ω_n/Ω_p of the neutrons with respect to the protons is also varied. Generally speaking, stars that are spun up without changing the total baryon number move upward and to the left in the figure. We find that we recover the so-called ''supramassive'' configurations first discussed by Cook *et al.* [33]. These are stars whose central densities go beyond the maximum allowed for stable, non-rotating configurations and yet still remain on the stable (upward) branches of their particular mass vs central density curves. These configurations are stablized by their rotation.

Figure 9 gives plots of the ratio of the polar [i.e., $R_p = R + \xi(R,0)$] to equatorial [i.e., $R_e = R + \xi(R,\pi/2)$] radii, versus the relative rotation rate Ω_n/Ω_p for the canonical backgrounds given in models I and II of Table I and assuming a proton rotation rate of the fastest known pulsar. Up to and including $\mathcal{O}(\Omega_{n,p}^2)$ we have

$$\frac{R_p}{R_e} = 1 + \frac{3}{2}\,\frac{\xi_2(R)}{R}. \tag{80}$$

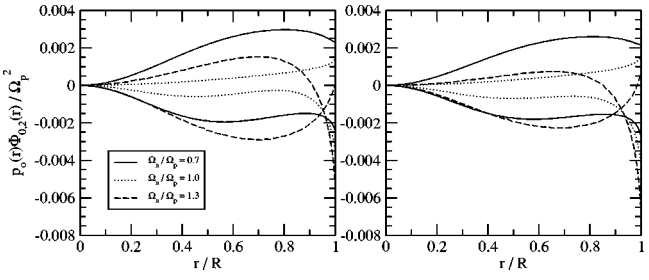

FIG. 7. The proton density corrections $p_o(r)\Phi_0(r)$—the 3 uppermost curves at $r/R = 1$—and $p_o(r)\Phi_2(r)$—the 3 lowermost curves at $r/R = 1$—vs r for models I (left panel) and II (right panel) of Table I. The relative rotation rates are varied ($\Omega_n/\Omega_p = 0.7$, 1.0, 1.3).

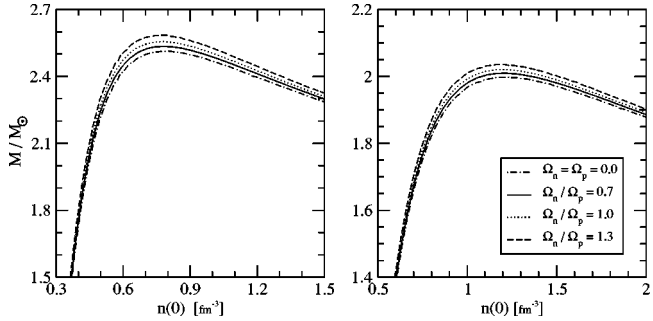

FIG. 8. The total mass as a function of central neutron number density for models I (left panel) and II (right panel) of Table I (using $\Omega_p = 3900$ rad/s). The relative rotation rates are also varied, i.e. $\Omega_n/\Omega_p = 0,\ 0.7,\ 1.0,\ 1.3$.

We see a general overall quadratic behavior in the relative rotation, which is expected for the slow rotation expansion. Also expected is the limiting value of $R_p/R_e = 1$ as $\Omega_n/\Omega_p \to 0$. Since the neutrons and protons have been constrained to vanish on the same surface, we do not find configurations like those of [12,14] whereby the neutrons, say, can extend out further than the protons.

Figure 10 is a graph of the Kepler (or mass-shedding) limit Ω_K versus the relative rotation rate for the canonical background configurations of Table I. Two competing factors are the amount of mass of the star that is in neutrons versus the relative rotation rate. For instance, for $\Omega_n/\Omega_p > 1$ the Kepler limit is seen to be essentially flat. This can be easily understood as a result of the fact that the neutrons represent nearly 90% of the mass of the system, and so the Kepler limit changes very little as the relative rotation is increased. Such behavior has also been seen in the analytical solution of Prix *et al.* [12], and the numerical results of Andersson and Comer [18]. The clear difference with the previous work is the general decrease in the Kepler limit as the relative rotation is decreased below one. Prix *et al.* and Andersson and Comer found that the Kepler limit increased monotonically as the relative rotation was decreased. They explained this as

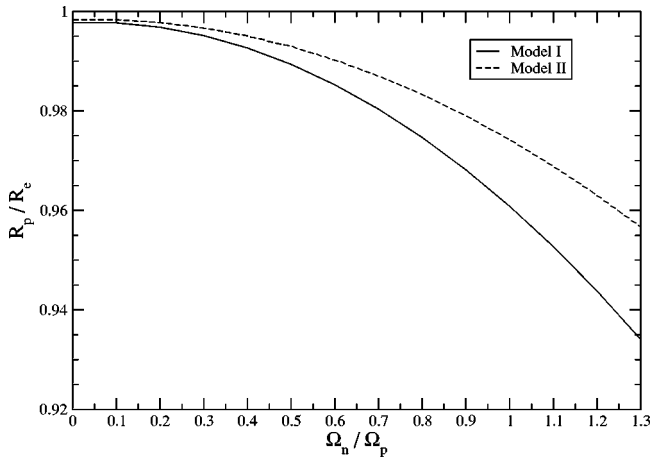

FIG. 9. The ratio R_p/R_e as a function of the relative rotation rate Ω_n/Ω_p for the canonical background configurations of models I and II of Table I and setting $\Omega_p = 3900$ rad/s.

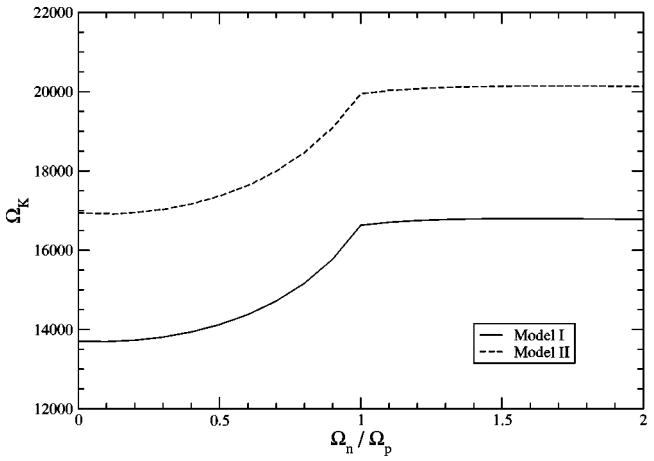

FIG. 10. The Kepler mass-shedding limit as a function of the relative rotation rate Ω_n/Ω_p for the canonical background configurations of models I and II of Table I.

a result of the fact that most of the mass is in the neutrons, and as the relative rotation is decreased, the Kepler limit is approaching the non-rotating value. As one can see in Fig. 10 eventually a minimum is reached, and beyond that the Kepler limit then starts to increase as the relative rotation is decreased. It just does not exhibit the monotonic increase of the earlier studies. The main differences with the two earlier studies are that here we use the mean field formalism for the equation of state—the previous two studies used simplified polytropes—and the entrainment is both relativistic and also has a nontrivial radial profile (cf. Figs. 2 and 3 of [8]), whereas the relevant entrainment parameter is kept constant in Prix *et al.* and taken to be zero in Andersson and Comer.

V. CONCLUSIONS

The earlier work of Comer and Joynt [8] laid the foundations for a fully relativistic approach to entrainment in superfluid neutron stars. They applied their formalism to first order in the rotational rates, and determined the impact of a relative rotation on the frame-dragging and the angular momenta of the two fluids. We have expanded on this work by extending the calculations to second order in the rotation rates, and have determined for the first time the maximum mass, shape, and Kepler limit using a fully relativistic formulation for entrainment and allowing a relative rotation between the two fluids.

An important extension of our work will be to include isotopic spin terms in the master function [16]. These are important for incorporating symmetry energy effects which tend to force baryonic systems to have as many protons as neutrons. Obviously nuclei tend to have equal numbers of neutrons and protons, and so this is why a symmetry energy term is an important addition to the equation of state. In terms of neutron stars, Prix *et al.* [12] have shown clearly that symmetry energy impacts rotational equlibria (e.g., ellipticity, the Kepler limit, and moment of inertia) as the relative rotation is varied.

The next application we have in mind is to study quasinormal modes on slowly rotating backgrounds. Andersson and Comer [34] (see also [13]) have shown that a suitably advanced gravitational wave detector should be able to see gravitational waves emitted during Vela or Crab-like glitches. Such observations could provide potentially unique information on the supranuclear equation of state and the parameters that govern entrainment. Another important application will be to study further the recently discovered two-stream instability [35,36]. It is the direct analog for superfluids of the instability of the same name known to exist in plasmas [37,38]. Finally, our results should also find some application in studies of vortex structure in neutron stars. Link [39] has suggested that free precession in neutron stars is not compatible with the protons behaving as a type II superconductor. This should be explored in more detail by allowing for the effect of entrainment.

ACKNOWLEDGMENTS

I thank N. Andersson for useful discussions and for providing aid with the code that served as the starting point for the research presented here. I also thank Bob Joynt for useful discussions and for pointing me in the direction of mean field theory for these entrainment calculations. The research presented here received support from NSF grant PHYS-0140138.

APPENDIX

For convenience, we list here the various matter coefficients that are required as input in the field equations:

$$\mathcal{A}|_{\rm o} = c_\omega^2 + \frac{c_\omega^2}{5\mu_{\rm o}^2}\left(2k_p^2 \frac{\sqrt{k_n^2+m_*|_{\rm o}^2}}{\sqrt{k_p^2+m_*|_{\rm o}^2}} + \frac{c_\omega^2}{3\pi^2}\left[\frac{k_n^2 k_p^3}{\sqrt{k_n^2+m_*|_{\rm o}^2}} + \frac{k_p^2 k_n^3}{\sqrt{k_p^2+m_*}}\Big|_{\rm o}^2 \right]\right) + \frac{3\pi^2 k_p^2}{5\mu_{\rm o}^2 k_n^3}\frac{k_n^2+m_*|_{\rm o}^2}{\sqrt{k_p^2+m_*|_{\rm o}^2}}, \tag{A1}$$

$$\mathcal{B}|_{\rm o} = \frac{3\pi^2\mu_{\rm o}}{k_n^3} - c_\omega^2\frac{k_p^3}{k_n^3} - \frac{c_\omega^2 k_p^3}{5\mu_{\rm o}^2 k_n^3}\left(2k_p^2 \frac{\sqrt{k_n^2+m_*|_{\rm o}^2}}{\sqrt{k_p^2+m_*|_{\rm o}^2}} + \frac{c_\omega^2}{3\pi^2} \times \left[\frac{k_n^2 k_p^3}{\sqrt{k_n^2+m_*|_{\rm o}^2}} + \frac{k_p^2 k_n^3}{\sqrt{k_p^2+m_*}}\Big|_{\rm o}^2 \right]\right) - \frac{3\pi^2 k_p^5}{5\mu_{\rm o}^2 k_n^6}\frac{k_n^2+m_*|_{\rm o}^2}{\sqrt{k_p^2+m_*|_{\rm o}^2}}, \tag{A2}$$

$$\mathcal{C}|_{\rm o} = \frac{3\pi^2\chi_{\rm o}}{k_p^3} - c_\omega^2\frac{k_n^3}{k_p^3} - \frac{c_\omega^2 k_n^3}{5\mu_{\rm o}^2 k_p^3}\left(2k_p^2 \frac{\sqrt{k_n^2+m_*|_{\rm o}^2}}{\sqrt{k_p^2+m_*|_{\rm o}^2}} + \frac{c_\omega^2}{3\pi^2} \times \left[\frac{k_n^2 k_p^3}{\sqrt{k_n^2+m_*|_{\rm o}^2}} + \frac{k_p^2 k_n^3}{\sqrt{k_p^2+m_*}}\Big|_{\rm o}^2 \right]\right) - \frac{3\pi^2}{5\mu_{\rm o}^2 k_p}\frac{k_n^2+m_*|_{\rm o}^2}{\sqrt{k_p^2+m_*|_{\rm o}^2}} + \frac{3\pi^2}{k_p^3}\sqrt{k_p^2+m_e^2}, \tag{A3}$$

$$\mathcal{A}^0_0|_{\rm o} = -\frac{\pi^4}{k_n^2 k_p^2}\frac{\partial^2\lambda_0}{\partial k_p \partial k_n} = c_\omega^2 + \frac{\pi^2}{k_p^2}\frac{m_*|_{\rm o}\dfrac{\partial m_*|_{\rm o}}{\partial k_p}}{\sqrt{k_n^2+{m_*|_{\rm o}}^2}}, \tag{A4}$$

$$\mathcal{B}^0_0|_{\rm o} = \frac{\pi^4}{k_n^5}\left(2\frac{\partial\lambda_0}{\partial k_n} - k_n\frac{\partial^2\lambda_0}{\partial k_n^2}\right) = c_\omega^2 + \frac{\pi^2}{k_n^2}\frac{k_n + m_*|_{\rm o}\dfrac{\partial m_*|_{\rm o}}{\partial k_n}}{\sqrt{k_n^2+{m_*|_{\rm o}}^2}}, \tag{A5}$$

$$\mathcal{C}^0_0|_{\rm o} = \frac{\pi^4}{k_p^5}\left(2\frac{\partial\lambda_0}{\partial k_p} - k_p\frac{\partial^2\lambda_0}{\partial k_p^2}\right) = c_\omega^2 + \frac{\pi^2}{k_p^2}\frac{k_p + m_*|_{\rm o}\dfrac{\partial m_*|_{\rm o}}{\partial k_p}}{\sqrt{k_p^2+{m_*|_{\rm o}}^2}} + \frac{\pi^2}{k_p}\frac{1}{\sqrt{k_p^2+m_e^2}}, \tag{A6}$$

where

$$\frac{\partial m_*|_{\rm o}}{\partial k_n} = -\frac{c_\sigma^2}{\pi^2}\frac{m_*|_{\rm o}k_n^2}{\sqrt{k_n^2+{m_*|_{\rm o}}^2}}\left(\frac{3m-2m_*|_{\rm o}}{m_*|_{\rm o}} - \frac{c_\sigma^2}{\pi^2}\left[\frac{k_n^3}{\sqrt{k_n^2+{m_*|_{\rm o}}^2}} + \frac{k_p^3}{\sqrt{k_p^2+{m_*|_{\rm o}}^2}}\right]\right)^{-1}, \tag{A7}$$

$$\frac{\partial m_*|_{\rm o}}{\partial k_p} = -\frac{c_\sigma^2}{\pi^2}\frac{m_*|_{\rm o}k_p^2}{\sqrt{k_p^2+{m_*|_{\rm o}}^2}}\left(\frac{3m-2m_*|_{\rm o}}{m_*|_{\rm o}} - \frac{c_\sigma^2}{\pi^2}\left[\frac{k_n^3}{\sqrt{k_n^2+{m_*|_{\rm o}}^2}} + \frac{k_p^3}{\sqrt{k_p^2+{m_*|_{\rm o}}^2}}\right]\right)^{-1}. \tag{A8}$$

The two functions $\mu_{\rm o}$ and $\chi_{\rm o}$ are the background values for the two chemical potentials:

$$\mu_{\rm o} = \frac{c_\omega^2}{3\pi^2}(k_n^3+k_p^3) + \sqrt{k_n^2+{m_*|_{\rm o}}^2},$$

$$\chi_{\rm o} = \frac{c_\omega^2}{3\pi^2}(k_n^3+k_p^3) + \sqrt{k_p^2+{m_{*\rm o}}^2}. \tag{A9}$$

Chemical equilibrium for the background means $\mu_{\rm o}=\chi_{\rm o}+\sqrt{k_p^2+m_e^2}$ must be imposed. Given a value for $k_n(0)$ then $k_p(0)$ can be determined. Using these then the initial value for the Dirac effective mass can be obtained from Eq. (77) so that Eq. (79) can be integrated.

[1] V. Radhakrishnan and R.N. Manchester, Nature (London) **244**, 228 (1969).
[2] A.G. Lyne, in *Pulsars as Physics Laboratories*, edited by R.D. Blandford, A. Hewish, A.G. Lyne, and L. Mestel (Oxford University Press, New York, 1993).
[3] P.E. Reichley and G.S. Downs, Nature (London) **222**, 229 (1969).
[4] G. Baym, C. Pethick, D. Pines, and M. Ruderman, Nature (London) **224**, 872 (1969).
[5] P.W. Anderson and N. Itoh, Nature (London) **256**, 25 (1975).
[6] M.A. Alpar, P.W. Anderson, D. Pines, and J. Shaham, Astrophys. J. **276**, 325 (1984).
[7] M.A. Alpar, P.W. Anderson, D. Pines, and J. Shaham, Astrophys. J. **278**, 791 (1984).
[8] G.L. Comer and R. Joynt, Phys. Rev. D **68**, 023002 (2003).
[9] H. Dimmelmeier, J.A. Font, and E. Müller, Astron. Astrophys. **393**, 523 (2002).
[10] S.W. Bruenn, K.R. De Nisco, and A. Mezzacappa, Astrophys. J. **560**, 326 (2001).
[11] F. Weber, *Pulsars as Astrophysical Laboratories for Nuclear and Particle Physics* (Institute of Physics Publishing, Bristol and Philadelphia, 1999).
[12] R. Prix, G.L. Comer, and N. Andersson, Astron. Astrophys. **381**, 178 (2002).
[13] N. Andersson, G.L. Comer, and D. Langlois, Phys. Rev. D **66**, 104002 (2002).
[14] R. Prix, J. Novak, and G.L. Comer, in *Proceedings of the 26th Spanish Relativity Meeting: Gravitation and Cosmology*, edited by A. Lobo, F. Fayos, J. Garriga, E. Gaztañaga, and E. Verdaguer (University of Barcelona, Barcelona, 2003), pp. 212–217.
[15] J.D. Walecka, *Theoretical Nuclear and Subnuclear Physics* (Oxford University Press, New York, 1995).
[16] N.K. Glendenning, *Compact Stars: Nuclear Physics, Particle Physics, and General Relativity* (Springer-Verlag, New York, 1997).
[17] G.L. Comer, D. Langlois, and L.M. Lin, Phys. Rev. D **60**, 104025 (1999).
[18] N. Andersson and G.L. Comer, Class. Quantum Grav. **18**, 969 (2001).
[19] A.F. Andreev and E.P. Bashkin, Sov. Phys. JETP **42**, 164 (1976).
[20] J. Sauls, in *Timing Neutron Stars*, edited by H. Ögelman and E.P.J. van den Heuvel (Kluwer, Dordrecht, 1989), pp. 457–490.
[21] M. Borumand, R. Joynt, and W. Klúzniak, Phys. Rev. C **54**, 2745 (1996).
[22] C.W. Misner, K. Thorne, and J.A. Wheeler, *Gravitation* (Freeman, San Francisco, 1973).
[23] B. Carter, in *Relativistic Fluid Dynamics*, edited by A. Anile and M. Choquet-Bruhat (Springer-Verlag, Berlin, 1989).
[24] G.L. Comer and D. Langlois, Class. Quantum Grav. **11**, 709 (1994).
[25] B. Carter and D. Langlois, Phys. Rev. D **51**, 5855 (1995).
[26] B. Carter and D. Langlois, Nucl. Phys. **B454**, 402 (1998).
[27] B. Carter and D. Langlois, Nucl. Phys. **B531**, 478 (1998).

[28] D. Langlois, A. Sedrakian, and B. Carter, Mon. Not. R. Astron. Soc. **297**, 1189 (1998).
[29] R. Prix, Phys. Rev. D **62**, 103005 (2000).
[30] G.L. Comer, Found. Phys. **32**, 1903 (2002).
[31] J.B. Hartle, Astrophys. J. **150**, 1005 (1967).
[32] J.L. Friedman, J.R. Ipser, and L. Parker, Astrophys. J. **304**, 115 (1986).
[33] G.B. Cook, S.L. Shapiro, and S.A. Teukolsky, Astrophys. J. **422**, 227 (1994).
[34] N. Andersson and G.L. Comer, Phys. Rev. Lett. **24**, 241101 (2001).
[35] N. Andersson, G.L. Comer, and R. Prix, Phys. Rev. Lett. **90**, 091101 (2003).
[36] R. Prix, G.L. Comer, and N. Andersson, Mon. Not. R. Astron. Soc. **348**, 625 (2004).
[37] D.T. Farley, Phys. Rev. Lett. **10**, 279 (1963).
[38] O. Buneman, Phys. Rev. Lett. **10**, 285 (1963).
[39] B. Link, Phys. Rev. Lett. **91**, 101101 (2003).